Received: 16 April 2024 | Revised: 28 June 2024 | Accepted: 25 July 2024

DOI: 10.1002/app.56109

RESEARCH ARTICLE

Applied Polymer SCIENCE WILEY

Impact of oxidized sucrose as a bio-based crosslinker on thermoformable films made from lupin protein isolate (*Lupinus angustifolius* L.)

Maximilian Maidl[1] | **Heidi Englberger**[1] | **Amirhossein Abbasnia**[2] | **Daniel Van Opdenbosch**[1] | **Cordt Zollfrank**[1]

[1]Biogenic Polymers, Technische Universität München, Straubing, Germany

[2]Chemistry of Biogenic Resources, Technische Universität München, Straubing, Germany

Correspondence
Cordt Zollfrank, Chemistry of Biogenic Resources, Technische Universität München, Straubing, Germany.
Email: cordt.zollfrank@tum.de

Funding information
Bayerisches Staatsministerium für Ernährung, Landwirtschaft und Forsten

Abstract

This study investigates the effect of oxidized sucrose (OS) on selected functional properties of cast films from lupin protein isolate (LPI). LPI with a protein content larger than 0.9 g g^{-1} was obtained by alkaline extraction and isoelectric precipitation from bitter narrow-leaved lupins (*Lupinus angustifolius* L.). OS was synthesized by vicinal diol cleavage using sodium periodate and was successfully characterized by Fourier-transform infrared-, ^{1}H-nuclear magnetic resonance spectroscopy, and aldehyde titration. Films were produced from heated (85°C, 30 min), alkaline (pH 10), aqueous solutions of LPI (0.1 mL^{-1}), glycerol (300 mg g^{-1} of LPI) and OS (25, 50, 75, and 100 mg g^{-1} of LPI). The effect of covalent crosslinking between OS and protein chains was studied by investigating mechanical properties, moisture content, total soluble matter, water vapor permeability, and protein solubility for all films. LPI films produced with the addition of OS showed increased mechanical performance as the tensile strength was increased from 3.5 up to 9.3 MPa and elongation at break values could be raised from 118% to 176%. Taken together with the facts that these films are thermoformable and show improved wet strength compared with control films, make them promising materials for sustainable packaging and short-term applications in agriculture and forestry.

KEYWORDS

bio-based crosslinker, functional properties, lupin protein, oxidized sucrose, protein-based materials

1 | INTRODUCTION

Due to their environment-friendly nature, biodegradability, and potential use in the packaging and agricultural industry, films from biopolymers are of substantial interest.[1] Biopolymers, such as polysaccharides and proteins, can be obtained from natural resources, secondary waste streams, or food processing waste, contributing to sustainability and a circular economy. Proteins show great film-forming ability, and unlike homopolymers

(e.g., polysaccharides), they are characterized by heterogeneous structures that permit various interactions and bonds that differ in position, type, and energy.[2] They can be considered as an alternative to non-biodegradable petroleum-based plastics since they are abundant, renewable, and biodegradable. They are promising materials, particularly in applications as bioplastic materials for mulch films, seed wraps, and packaging films, where high biodegradability is required after the use phase.[3-6] However, there are some limitations in applications due to low strength, elongation at break and toughness values as well as high sensitivity to moisture.[7]

Since proteins from different sources differ in type, amino acid composition, and conformation, this strongly affects material properties. For this reason, different plant proteins such as pea protein, zein, and wheat gluten were investigated for material production.[8–10] However, soy protein in particular, as an abundant raw material, has been intensively researched for bioplastic preparation.[11,12] Soybeans are grown in large-scale monocultures and require good soil moisture and low salinity levels in the soil and irrigation water. Other legume crops, such as lupins, are favored in drier or saline-affected areas that are inappropriate for soybean cultivation. Lupin cultivation offers a range of environmental benefits, as it mobilizes soil-bound phosphate and has a high nitrogen fixation rate into the soil at 150–200 kg ha^{-1}.[13] To our knowledge, crosslinked films from lupin protein have not been produced and studied so far and therefore we expand the range of renewable resources for producing advanced biopolymer films.

Despite similarities in the composition of soy and lupin protein, it could be shown that they behave fundamentally differently in terms of gel formation and consistency. Berghout et al. hypothesized that the thermal stability of lupin protein isolate (LPI) is related to its high sulfhydryl content and, thus, a large number of intramolecular interactions that could lead to a more stable structure.[14] An investigation using differential scanning calorimetry of the 7S and llS globulin fractions extracted from lupin and soybeans by Sousa et al. showed that they exhibit different denaturation behaviors.[15]

Lupin (*Lupinus* L., Fabaceae) is a species-rich legume distributed in a wide range of geographical regions. The seed proteins of *Lupinus angustifolius* L. used in this study consist mainly of globulins and albumins with a mass ratio of 9 to 1. Only small amounts of other protein fractions, such as prolamins and glutelins, were detected.[16,17] The seed storage proteins are classified into conglutin α (11S legumin-like globulins), conglutin β (7S vicilin-like globulins), conglutin γ (7S basic globulins), and conglutin δ (2S sulfur-rich albumins). Conglutins α and β together make up to 90% of total globulins, while γ and δ constitute the remaining fraction.[16,18] Therefore, mainly conglutins α and β are responsible for film formation in LPI films.

Films from plant protein can be produced by solution casting or compression molding.[19] A few groups investigated lupin proteins of different species as raw material for film production: Chango et al. reported films from thermocoagulated protein fractions from *L. albus* and *L. luteus* for food applications.[20] A study by Hopkins et al. focused on the effect of glycerol on selected properties of cast films from different legume protein concentrates. They proposed that protein purity and intrinsic factors significantly impact the mechanical performance of films based on lupin protein concentrate.[21] Cast films from LPI (*L. albus*) for food applications were produced by Alsadi et al. at different pH values, and their effect on material properties was investigated.[22]

Until now, numerous attempts have been made to improve the mechanical properties and moisture stability of soy protein films by physical, chemical, enzymatic, or physicochemical methods.[7,23] Due to the hydrophilic nature of most plant proteins, there are limited possibilities to eliminate moisture sensitivity. Kamada et al. showed that exposure to acetic acid and ultrasonication to plant protein solutions and the subsequent preparation of films can increase mechanical strength and moisture stability.[24] Blending plant protein materials with other biopolymers, such as cellulose or starch, is another approach to modify these material properties.[25,26] Chemical crosslinking of plant protein with formaldehyde, glutaraldehyde, or glyoxal has been an effective method to increase the mechanical performance of protein films. However, using formaldehyde and its analogues is highly questionable due to its toxicity and cancerogenic nature.[27] Sugar-based polyaldehydes, such as oxidized sucrose (OS) or dialdehyde starch, were investigated as bio-based crosslinking agents with low toxicity and high reaction efficiency for the preparation of biopolymer films.[3,28-30] Films from soy protein isolate (SPI) and corn protein crosslinked with OS were already investigated[31,32]. Both studies pointed out that the addition of OS increased mechanical strength and lowered the water sensitivity of produced films.

The covalent crosslinking between proteins and aldehydes is very complex and poorly understood. Different reaction mechanisms are suggested depending on pH value, protein type, and crosslinker. However, in the literature, it is widely accepted that the crosslinking of protein is mediated by aldehydes through unprotonated lysine residues and the amino groups of *N*-terminal amino acids[33,34] (Figure 1). Under basic conditions, it was shown that Schiff base formation with subsequent release of water is very likely to occur.[35] Lupin protein,

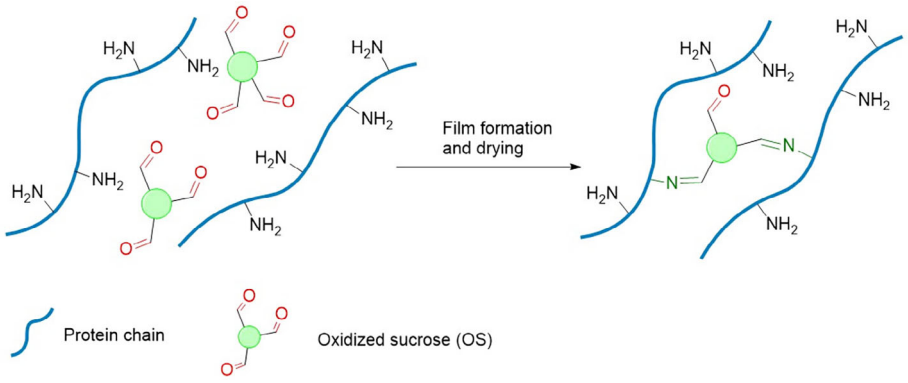

FIGURE 1 Schematic representation of the presumed crosslinking reaction between primary amino groups and OS during film formation. OS, oxidized sucrose. [Color figure can be viewed at wileyonlinelibrary.com]

as most legume protein, contains high levels of lysine and arginine and is therefore suitable for aldehyde crosslinking.[16,36]

This article aims to demonstrate that lupin protein can be considered a raw material for biopolymer films. Further, we hypothesize that the addition of OS significantly impacts the material properties of LPI films by covalent crosslinking. In addition, we show that non-crosslinked and crosslinked LPI films can be processed by thermoforming, which opens up new application fields for protein-based materials. We also show the extent to which crosslinking with OS affects biodegradation in soil.

2 | MATERIALS AND METHODS

2.1 | Materials

Lupin seeds from bitter narrow-leaved lupins were provided by ESKUSA GmbH (Parkstetten, Germany). D(+)-sucrose (≥99.5%) and sodium meta periodate (≥99.0%) were purchased from Sigma Aldrich. Barium dichloride (99.9%) and hydroxylamine hydrochloride (99%) were obtained from Alfa Aesar. Sodium hydroxide, hydrochloric acid (35%), and glycerol (≥99.5%) were purchased from Carl Roth. *N*-hexane (≥95%, technical) was obtained from VWR and sodium azide (99%) from PanReac AppliChem.

2.2 | Isolation of lupin protein

Whole lupin seeds were ground in an A11 basic analytical mill (IKA, Germany). The resulting lupin flour (LF) was defatted in a soxhlet apparatus by extraction with *n*-hexane at 78°C for at least 4 h. The defatted LF (DLF) was suspended in distilled water (100 g L^{-1}), and the pH value was kept at 8.5 ± 0.1 with 1 M NaOH for 3 h under constant stirring at room temperature. The slurry was centrifuged at 3828*g* for 30 min, and the pellet was discharged. The supernatant was precipitated by adding 1 M HCl at pH 4.5. The precipitate, containing LPI, was recovered by centrifugation, washed with distilled water, and freeze-dried.

2.3 | Protein content and recovery

The nitrogen content (c_N) of LF, DLF, and LPI and the carbon content of the LPI control film and the LPI/OS100 film were measured by a EuroEA-Elemental Analyzer (Eurovector, Italy). Exactly 1–3 mg of the samples were analyzed in tin crucibles. The protein content (c_P) was calculated using the nitrogen-to-protein factor 6.25. Protein contents of the DLF and LPI were used to calculate the protein recovery (r_P) by using the following formula:

$$r_P = \frac{m_{LPI} \cdot c_{p,LPI}}{m_{DLF} \cdot c_{p,DLF}}. \quad (1)$$

2.4 | Oxidation of sucrose

OS was prepared according to a modified procedure by Kono et al.[28] Sucrose (6.00 g, 17.5 mmol) and sodium periodate (11.3 g, 52.5 mmol) were dissolved in 200 mL distilled water and the reaction mixture was stirred for 24 h at room temperature. Then, barium dichloride (6.42 g, 26.2 mmol) was added and the mixture was stirred in an ice bath for 1 h to allow complete precipitation of barium iodate. The mixture was filtered to obtain the supernatant solution containing OS. The supernatant was passed through a mixed bed ion exchange resin (Amberlite MB20, Sigma Aldrich) to remove formic acid, remaining barium dichloride, and periodate ions. The resulting solution was freeze-dried to obtain OS as a white powder.

2.5 | Film preparation

The film-forming solutions were prepared by stirring 0.1 g mL^{-1} LPI and 300 mg g^{-1} glycerol in distilled water for 15 min. The pH values of the solutions were adjusted to 10.0 ± 0.1 with 1 M NaOH and were stirred for an additional 15 min. Subsequently, the solutions were homogenized for 1 min at 10,000 rpm using a T 25 digital Ultra-Turrax homogenizer (IKA, Germany). The dispersions were then heated in a water bath at 85°C for 30 min and filtered through Miracloth (typical pore size: 22–25 μm, Merck) to remove foam and undissolved impurities. Afterward, OS (25, 50, 75, and 100 mg g^{-1} of LPI) was added under constant stirring. After the complete dissolution of the additive, 50 mL of the solutions were poured into rectangular, 15 × 25 cm PDMS molds. Cast solutions were allowed to dry at room temperature for at least 48 h, were peeled off, and stored in an environmental chamber (T = 23°C, relative humidity = 50%) until further use.

2.6 | Fourier-transform infrared spectroscopy

Fourier-transform infrared (FTIR) spectra were recorded using a Frontier MIR spectrometer (PerkinElmer, USA) performed with an attenuated total reflection (ATR) diamond. The spectra were recorded between 4000 and 525 cm^{-1} with a resolution of 4 cm^{-1} and 16 scans.

2.7 | Nuclear magnetic resonance spectroscopy

For the structural characterization of OS, a ^{1}H-nuclear magnetic resonance spectrum (^{1}H NMR spectrum) was acquired on an ECS-400 NMR (Jeol, Japan). The evaluation was performed by MestReNova v 14.2.3 (Mestrelab Research, Spain). OS was analyzed in D_2O (VWR, France) at 25°C, and the spectrum was measured with 32 scans.

2.8 | Aldehyde quantification of OS by titration

Aldehyde quantification was conducted according to a modified titration procedure by Wing and Willet,[37] who determined the carbonyl content of oxidized starch. Typically, 0.1 g of OS was dissolved in 100 mL of distilled water. The solution was adjusted to pH 3.2 with 0.1 M HCl, and 30 mL of 5.0 g L^{-1} hydroxylamine solution in 0.1 M NaOH were added. The solution was heated to 40°C in a water bath for 2 h and titrated rapidly back to pH 3.2 with 0.1 M HCl. Sucrose in distilled water was used as a control. All titrations were performed in triplicates. The aldehyde content (c_a) was calculated according to Equation (2):

$$c_a = \frac{(V_{sample} - V_{control}) \cdot c_{HCl}}{m_{sample}}. \quad (2)$$

2.9 | Material characterization of LPI films

2.9.1 | Mechanical testing

Film samples were cut into strip-shaped specimens (type 2, DIN EN ISO 527-3:2018). They were conditioned in an environmental chamber at 23°C and relative humidity = 50% for 72 h before testing. At least five replicates were tested for each formulation on a SmartTENS 20 (Emmeram Karg Industrietechnik, Germany). Initial grip separation was set at 50 mm and cross-head speed was set at 10 mm min^{-1}. Tensile strength (R_m), elongation at break (A_t), Young's modulus (E), and work of fracture (W_f) were calculated from the measured stress (σ)–strain (ε) data. R_m and A_t were obtained by the following equations:

$$R_m = \max(\sigma), \quad (3)$$

$$A_t = \max(\varepsilon). \quad (4)$$

Further, E was calculated from the linear elastic area in the starting region of the stress–strain curve with Equation (5).

$$E = \frac{d\sigma_{el}}{d\varepsilon_{el}}. \quad (5)$$

By integration of the stress–strain curve the W_f as a measure for the toughness of the film could be obtained as follows:

$$W_f = \int_0^{A_t} \sigma d\varepsilon. \quad (6)$$

2.9.2 | Moisture content

Film samples were collected after conditioning, cut into 2 × 2 cm squares, and weighed before and after drying in an oven at 105°C for 24 h. Moisture content values were determined in triplicate as the difference between the weights before and after drying and were expressed as a ratio referred to the initial weight.

2.9.3 | Total soluble matter

The total soluble matter (TSM) of the films was determined according to a modified method proposed by Kunte et al.[38] Three 2×2 cm film samples were immersed in 50 mL distilled water, a small amount of sodium azide was added to prevent biodegradation, and the system was slowly stirred at room temperature for 24 h. After filtration of the samples, the non-solubilized matter was dried in an oven at 105°C for 24 h to determine the weight of the water-insoluble fraction as a ratio referred to the initial weight.

2.9.4 | Water vapor permeability

For the calculation of the water vapor permeability (WVP) of the produced films, the water vapor transmission rate (WVTR) has to be measured. WVTR was determined gravimetrically according to ASTM E96 in triplicates. Each film specimen was sealed over a circular opening with an area of 10 cm^2 in a permeability cup filled with distilled water. The cups were placed in a climate chamber at 23°C and 50% relative humidity. When a constant mass loss was reached (after about 1 h), eight weight measurements were made over a period of 72 h. The data points were plotted as a function of time and the slope was calculated by linear regression (OriginLab, USA). WVTR was calculated as follows:

$$\mathrm{WVTR} = \frac{\Delta m}{\Delta t \cdot A}. \tag{7}$$

WVP was calculated according to the following equation:

$$\mathrm{WVP} = \frac{\mathrm{WVTR} \cdot d}{\Delta p}, \tag{8}$$

where d is the mean film thickness and Δp is the partial water vapor pressure difference between the two sides of the film specimen.

2.9.5 | Film thickness

Before tensile tests and WVTR measurements, the film thickness was measured with a digital, hand-held micrometer. Three thickness measurements were taken on each tensile test specimen and WVTR specimen. The mean thickness values were used for further calculations.

2.9.6 | Protein solubility

Preweighed film samples from 5 to 10 g were immersed in 1 mL PBS-buffer and stirred for 24 h at room temperature. After centrifugation, the protein concentrations of the supernatants were determined by a Bradford assay in triplicates using bovine serum albumin as standard protein for the calibration. The protein solubility was expressed as a ratio referred to the protein content in the LPI samples.

2.10 | SDS-PAGE

The effect of OS on the molecular weights of the proteins present in LPI were investigated using a sodium dodecyl sulfate-polyacrylamide gel electrophoresis (SDS-PAGE). Due to the poor solubility of the films crosslinked with OS, the crosslinking process was recreated. A LPI solution with a concentration of 2 mg mL^{-1} and 100 mg g^{-1} of OS was prepared. The crosslinking occurred at room temperature under gentle agitation for 20 min. The proteins were precipitated with cold acetone, and the pellet was dissolved in MilliQ water. This process was performed with (lane 3) and without (lane 2) the addition of OS. As an additional control, freeze-dried LPI (lane 1) was dissolved directly in MilliQ water. The samples were heated at 60°C for 5 min under shaking. They were centrifuged, and 20 µL of each sample was loaded into each pocket of the gel. After the electrophoresis, the gel was stained with Coomassie Brilliant Blue G250 and washed with water. The molecular weights of the protein ladder ranged from 10 to 200 kDa.

2.11 | Biodegradation testing

Aerobic biodegradation of organic matter results in conversion to CO_2, biomass, and water. Therefore, the produced amount of CO_2 is a good measure for biological degradation. For the biodegradation testing, a modified method by Eckel et al. was applied.[39] The soil used for biodegradation was obtained from a local composting facility (Zweckverband Abfallwirtschaft Straubing Stadt und Land, Straubing, Germany). Organic waste residues were removed from the soil using a sieve with a mesh size of 1 mm. To improve the biodegradation conditions, the moisture content of the soil was adjusted until a loose and moist soil consistency was achieved. The released CO_2-amount was absorbed in 20 mL of 1 M KOH solution, which was placed in the gas space without contacting the soil. Before testing, the CO_2 produced by the soil

without samples was analyzed to ensure that all the jars emitted the same amount of CO_2.

Four jars of soil were used as blanks, four jars of cellulose powder (Sigma Aldrich, USA) were used as positive controls, and three jars of polypropylene were used as negative controls. All materials were tested in triplicate. The film samples were ground by using an analysis mill (IKA, Germany). In each jar, 0.9 g of the sample was homogeneously distributed in the soil. Fresh KOH solution was added to a beaker placed over the soil and was titrated as the pH approached 9 to ensure that CO_2 uptake remained quantitatively valid. The samples were titrated at room temperature for several times over a period of 91 days. The CO_2 absorbed m_{CO_2} (sample) corresponds to the volume of HCl between the two inflection points of the pH titration curve at pH 8.1 and 3.9 and was calculated as follows:

$$n_{HCl} = n_{CO_2}, \tag{9}$$

$$m_{CO_2}(\text{sample}) = c_{HCl} \cdot V_{HCl} \cdot M_{CO_2}. \tag{10}$$

The calculated average CO_2 weight of all blanks was subtracted from each jar. The carbon content of the materials was determined in triplicate by elemental analysis and the theoretical CO_2 production $m_{CO_2}(\text{theoretical})$ was calculated as follows:

$$m_{CO_2}(\text{theoretical}) = \frac{m_C}{M_C} \cdot M_{CO_2}. \tag{11}$$

The proportion of biological degradation after 91 days D_{91d} was calculated by forming the ratio between $m_{CO_2}(\text{sample})$ and $m_{CO_2}(\text{theoretical})$ as shown in Equation (12).

$$D_{91d} = \frac{m_{CO_2}(\text{sample})}{m_{CO_2}(\text{theoretical})}. \tag{12}$$

2.12 | Thermoforming of LPI films

To demonstrate the thermoforming process, a custom-made device was utilized, in which circular LPI films with a diameter of >35 mm could be clamped. The LPI films were heated by placing the device for 2 min in a drying oven at 150°C. As a plug, the lid of a centrifuge tube with a diameter of 34 mm and a height of 13 mm was used. The device was removed from the oven, and the plug was slowly pressed into the LPI film. After a weight of 2.5 kg has been placed on the plug, the system was allowed to cool for 5 min. The thermoformed component based on LPI could then be removed from the device.

2.13 | Statistical analysis

All data were obtained at least in triplicate ($n = 3$) and expressed as mean ± standard deviation. The data were subjected to an one-way analysis of variance (ANOVA) by SPSS software (SPSS Statistics 29.0, IBM). Post hoc multiple comparisons were determined by the Scheffé test with the level of significance set at $P = 0.05$.

3 | RESULTS AND DISCUSSION

3.1 | Isolation of lupin protein

The prepared LPI was obtained as yellow powder and a protein content of 0.93 g g^{-1} based on dry matter was determined. From the protein content of the DLF of 0.93 g g^{-1}, a protein recovery rate (r_p) of 46% was calculated. This value is also in the size range of the r_p of Chew et al. and Muranyi et al. (59% and 29%), who applied the alkaline extraction-isoelectric precipitation method on narrow-leaved lupin seeds.[17,40] The alkaline extraction allowed the solubilization of the vast majority of lupin proteins, namely conglutins α, β, and δ. The isoelectric precipitate contains mainly these three conglutins, whereas conglutin γ remains in the supernatant.[13,41]

Figure 2 shows the FTIR spectra of LF, DLF, and LPI. All spectra show an absorption band at 3286 cm^{-1}, which can be attributed to O—H stretching. The FTIR spectra of LPI show similar absorption peaks as spectra obtained from other legume proteins.[42] The characteristic Amide I band (1700–1600 cm^{-1}) arises predominantly from the vibration of the C═O stretching of the protein backbone. The Amide II band (1580–1510 cm^{-1}) results mainly from N—H bending vibration and from C—N stretching vibration. The FTIR spectrum of LF shows further characteristic absorption peaks at 2925, 2855, and 1745 cm^{-1}, which are derived from contained lipids. Therefore, the intensities of these bands are decreasing after defatting of LF.[43]

3.2 | Oxidation of sucrose

The vicinal diol cleavage of sucrose using sodium periodate has been the focus of numerous research.[28,44,45] The unspecific oxidation of sucrose gives a complex mixture of isomeric acetals containing up to four aldehyde groups. By the selection of suitable solvent systems and reaction parameters, the selectivity toward highly

oxidized products can be increased.[44] In this study, OS was obtained as a white powder and showed good solubility in water, ethanol, and dimethyl sulfoxide. The aldehyde content per mass of OS was determined by titration with hydroxylamine solution, resulting in 11.0 mmol g^{-1}. The fact, that the theoretical aldehyde content of the tetraaldehyde is 12.3 mmol g^{-1},[28] indicates a high degree of oxidation of the produced OS. Therefore, increased selectivity of the sucrose oxidation by changing reaction parameters was not considered relevant for this work.

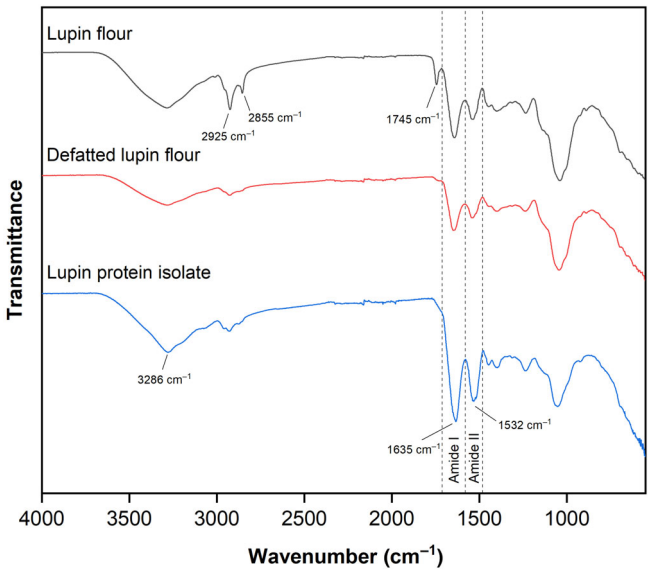

FIGURE 2 FTIR spectra of LF, DLF, and LPI. The spectra are vertically shifted for better readability. DLF, defatted lupin flour; LF, lupin flour; LPI, lupin protein isolate. [Color figure can be viewed at wileyonlinelibrary.com]

Figure 3a shows the FTIR spectra of sucrose and OS. In the FTIR spectrum of sucrose, absorption bands derived from OH—stretching vibration at 3559, 3382, and 3325 cm^{-1} can be observed. Peaks attributed to CH—stretching vibration at 2941 cm^{-1} and C—O—C stretching vibration at 1049, 988, and 907 cm^{-1} are further present in the spectrum. Due to oxidation, the peak at 3559 cm^{-1} in the FTIR spectrum of OS disappears, and two new peaks at 1728 and 1634 cm^{-1} are formed. They can be assigned to the C═O stretching vibration of the aldehyde groups and O—H— bending vibration of bound water.[45] These findings state that vicinal hydroxyl groups were oxidized into free aldehyde groups and therefore, the oxidation was considered successful.

Due to the different isomeric structures of OS, the ^{1}H NMR spectrum gives a complex resonance pattern with overlapping signals, which can not all be unambiguously determined. But according to the literature, the peak at 8.2 ppm can be assigned to the protons of free aldehyde groups upon oxidation.[45] Proton signals derived from intramolecular acetals appear from 4.6 to 5.4 ppm. These acetal bonds can be formed by the reaction of aldehyde groups with remaining hydroxyl groups. As the NMR spectra were recorded in D_2O, proton signals of hydroxyl groups cannot be observed due to rapid deuterium exchange. The proton peaks between 3.2 and 4.2 ppm can refer to —CH and —CH_2. The findings of the ^{1}H NMR experiments confirm that the oxidation of sucrose was achieved. However, its exact molecular structure and isomeric composition would require additional analysis. This is not considered necessary here because OS is expected to act as a crosslinking agent due to its high aldehyde content.

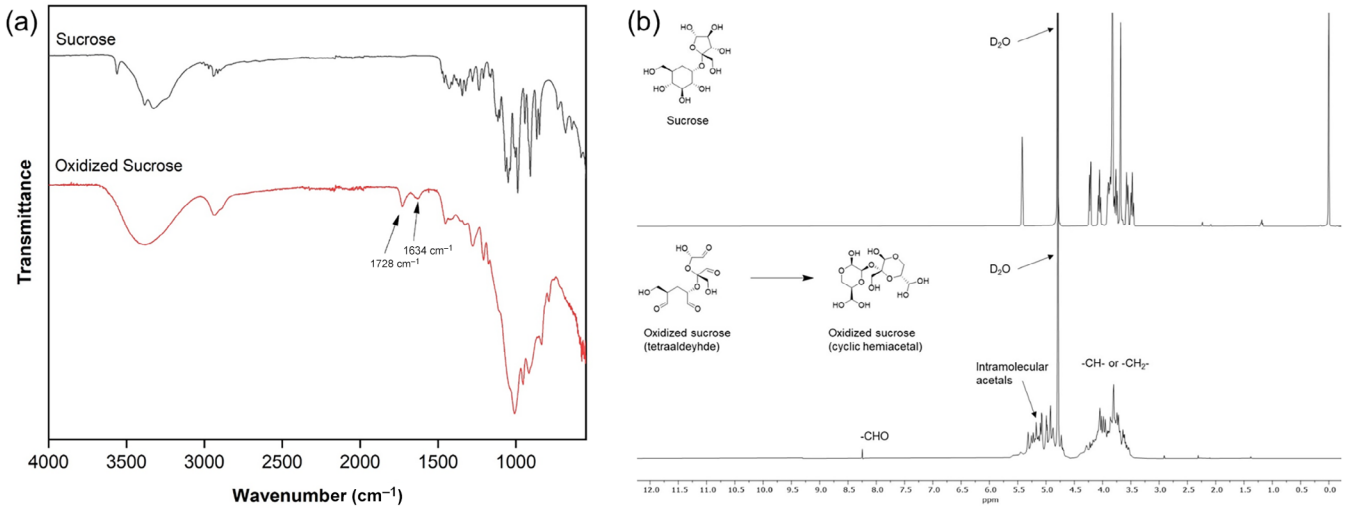

FIGURE 3 FTIR spectra (a) and ^{1}H NMR spectra (b) of sucrose and OS measured in D_2O with two exemplary structures of OS. The FTIR spectra are vertically shifted for better readability. NMR, nuclear magnetic resonance; OS, oxidized sucrose. [Color figure can be viewed at wileyonlinelibrary.com]

3.3 | Effect of OS on the material properties of LPI films

The preparation of LPI films using different amounts of OS (25, 50, 75, and 100 mg g^{-1}) and 300 mg g^{-1} of glycerol was carried out by solution casting. The thickness of the obtained films varied between 100 and 150 µm. The films were flexible, transparent, and the coloration varied from yellowish to orange/brown. With an increasing amount of OS color intensity increases and a slight browning occurs due to Maillard reaction products between carbonyl- and amino-containing compounds.[46] To assess the effect of crosslinking, different material properties of the films were investigated.

Mechanical properties were evaluated by R_m, A_t, E, and W_f, as a measure of toughness. Before tensile testing, the film specimens were conditioned at 23°C and relative humidity = 50%, as the water content of biopolymer films readily changes with ambient humidity through sorption/desorption phenomena. Water acts as natural plasticizer and strongly affects the film properties.[10,47] In Figure 4 typical stress–strain curves of the LPI control film and a LPI/OS100 film are shown. The different course of the two curves illustrates the effect of the addition of OS on the mechanical behavior. OS is a low molecular crosslinker and therefore we suggest that it can easily migrate between protein chains and form crosslinks. These crosslinks most likely refer to imine bonds that are formed by highly reactive aldehyde groups with lysine, histidine, and arginine, but also crosslinks with free cysteine side chains are conceivable.[48] As shown in Figure 5, the LPI control film without the addition of OS had a R_m of 3.5 MPa and an A_t value of 118% ± 7%. The high stretchability of the LPI films derives from the addition of glycerol: In preliminary tests 300 mg g^{-1} of glycerol was selected as adequate plasticizer amount to produce comparable films under fluctuating ambient conditions (temperature, relative humidity). Lower amounts (<200 mg g^{-1}) of glycerol made the films brittle, while higher amounts (>400 mg g^{-1}) resulted in sticky films.

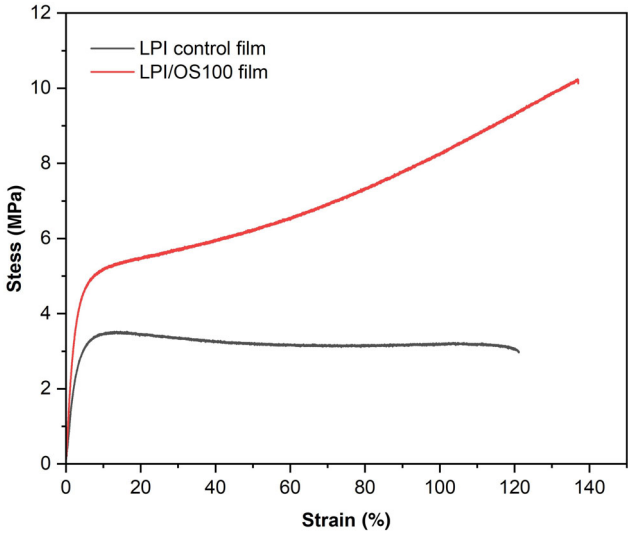

FIGURE 4 Typical stress–strain curves of LPI film and LPI film with 100 mg g^{-1} OS. LPI, lupin protein isolate; OS, oxidized sucrose. [Color figure can be viewed at wileyonlinelibrary.com]

R_m values increase almost up to a substantial threefold from 3.5 to 9.3 MPa with the addition of OS compared with the LPI control film. It seems, as a maximum R_m value for this system can be reached between 50 and 100 mg g^{-1} OS. A similar increase in R_m was reported by Liu et al., who invesigated SPI films modified with OS, they could achieve a doubling of the R_m by adding 100 mg g^{-1} of OS to the film forming solution.[49] In another study, the R_m of zein-based films could be increased from 10 up to 16 MPa by the addition of a bio-based polyaldehyde.[32] However, the comparability of the absolute values between the studies is limited, as both, the protein types and the quantity and/or type of plasticizers differ. Surprisingly, increasing OS concentration resulted in an initial increase of A_t from 118% to 176%. This significant increase of A_t with 25 mg g^{-1} OS likely results from an increase of cohesiveness of a less dense crosslinked protein network in the films. But it can also dervive from a plasticizing effect of OS by forming hydrogen bonds with the biopolymer matrix.[23] However, with increasing OS concentration and therefore inducing a stiffer network, the A_t values of the films are constantly decreasing again. In the aforementioned studies, both groups reported of decreasing A_t values when crosslinkers were added but they did not observe an inital increase of A_t compared with control films.[32,49]

All LPI films modified with OS have higher W_f values between 7 and 9 MJ m^{-3} and therefore a more ductile character than the control films. Similar observations were made for SPI films crosslinked with OS or DAS.[50,51] In Figure 5d one can anticipate a slight decrease in W_f with increasing OS content. In general, as molecular weight increases, which is achieved via covalent crosslinking, the toughness increases.[52] If the crosslinking density continues to increase by the addition of a higher amount of OS, these chemical links reduce molecular conformations attainable under stress and, therefore, decrease toughness values again.[53] The formed covalent crosslinks between protein chains act against deformation, which leads to high stiffness, which can be seen in the almost linear increase in E values (Figure 5c).[23]

Moisture sensitivity and the WVP of biopolymer films are highly relevant for their application in the packaging or agricultural sector. Table 1 shows the MC, TSM, and

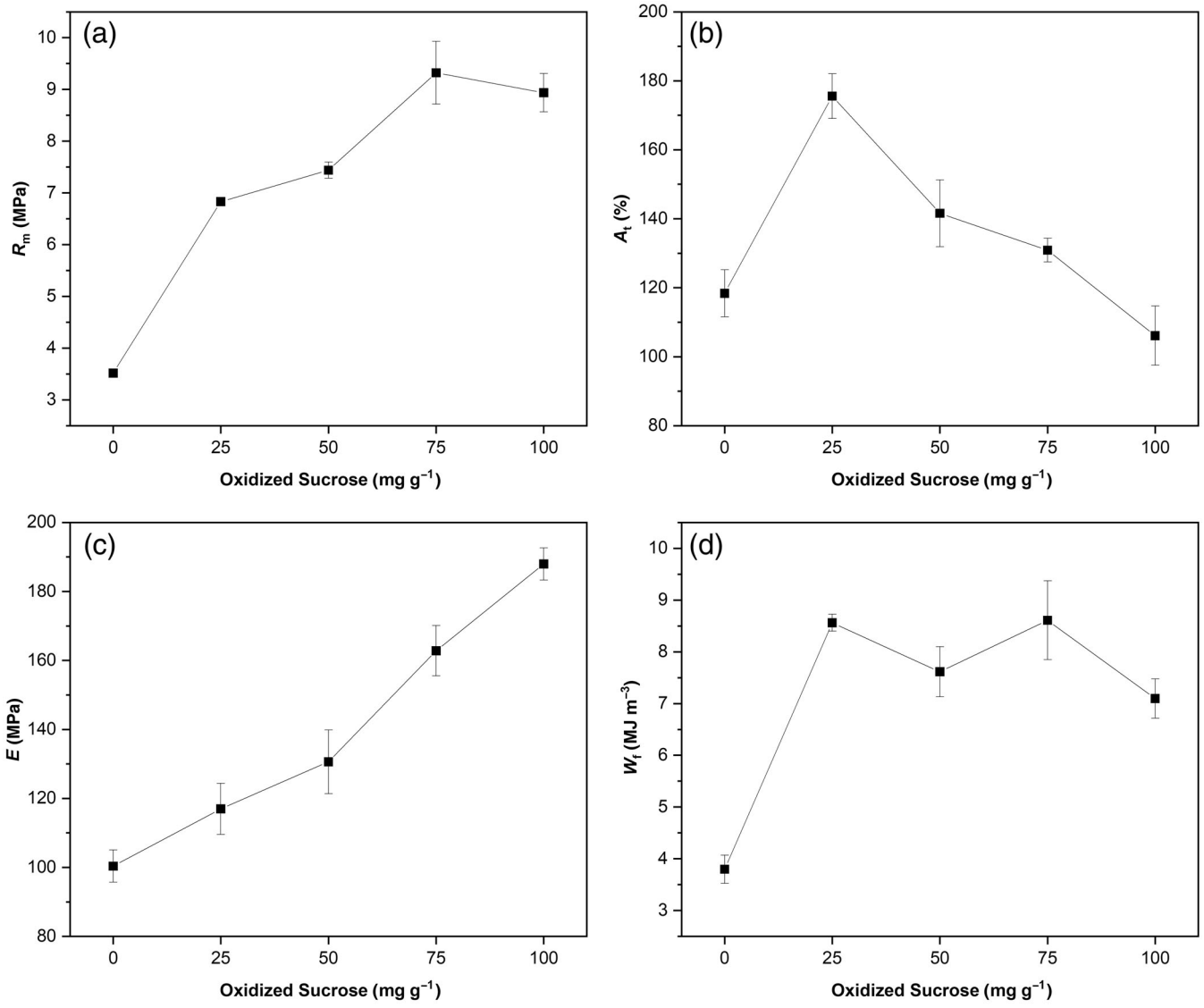

FIGURE 5 Plots of R_m (a), A_t (b), E (c), and W_f (d) of LPI films with different amounts of OS. LPI, lupin protein isolate; OS, oxidized sucrose.

TABLE 1 Moisture content (MC), total soluble matter (TSM), and water vapor permeability (WVP) of LPI-based films with different amounts of OS.

OS (mg g^{-1})	MC (mg g^{-1})	TSM (mg g^{-1})	WVP 10^{10} (g s^{-1} m^{-1} Pa^{-1})
Control	141 ± 3^{ab}	522 ± 3^{a}	1.48 ± 0.16^{a}
25	154 ± 1^{bc}	386 ± 9^{b}	1.41 ± 0.08^{ab}
50	157 ± 6^{c}	378 ± 44^{b}	1.13 ± 0.14^{b}
75	149 ± 1^{abc}	373 ± 3^{b}	1.38 ± 0.06^{ab}
100	140 ± 5^{a}	377 ± 2^{b}	1.16 ± 0.12^{b}

Note: Two means followed by the same letter in the same column are not significantly ($P > 0.05$) different based on the post hoc Scheffé test.
Abbreviation: OS, oxidized sucrose.

WVP for control films and films from LPI and different amounts of OS. All MC values are in the same range, and almost no significant differences were detected among control and LPI/OS films with varying amounts of added OS. This means that crosslinking by OS had only a marginal influence on the moisture uptake of LPI-based films and is in agreement with previous studies on films based on soy and zein proteins.[32,49] The TSM of the LPI films is mainly based on water, glycerol, and soluble protein fractions. As the values for the TSM of LPI/OS films

reduced approximately by 30% compared with control films, this indicates an increase in water-insoluble fractions. These fractions may derive from crosslinked protein complexes formed due to the addition of OS or retention of glycerol within the matrix. This significant effect of lower film solubilities by the addition of chemical crosslinkers was also emphasized by previous studies.[7]

Examination of the WVP of produced LPI films shows that all values are in the size range of WVP values of other protein-based films.[54] But a slight trend toward lower values can be observed when increasing OS concentration. By the addition of OS, covalent crosslinks are formed that can reduce the spacing between protein chains and affect the macromolecular arrangement in the films resulting in the observed slight reduction in WVP.[48] But as the hydrophilic character of the macromolecule did not change severely by crosslinking, we presume, that this plays a more crucial role.

TABLE 2 Protein solubility in PBS buffer determined by the Bradford assay method.

Sample	Protein solubility (mg g^{-1})
LPI	338.6 ± 3.7^{a}
LPI control film	155.2 ± 2.6^{b}
LPI/OS25 film	12.5 ± 1.6^{c}
LPI/OS50 film	2.9 ± 0.2^{d}
LPI/OS75 film	2.0 ± 0.1^{d}
LPI/OS100 film	1.7 ± 0.2^{d}

Note: Two means followed by the same letter in the same column are not significantly ($P > 0.05$) different based on the post hoc Scheffé test.

To investigate the crosslinking between protein chains in LPI, we determined the protein solubility in PBS buffer of produced films with the Bradford assay method. As shown in Table 2, the protein solubility of the control LPI film at 155 ± 3 mg g^{-1} is less than half as large as the maximum protein solubility of freeze-dried LPI in PBS buffer. This difference can be explained by the sample geometry and structural changes during the film formation. Adding OS to the film-forming solutions yields films with significantly reduced protein solubility in PBS buffer. For all the films, modified with OS, the protein solubility values were determined below 12 ± 2 mg g^{-1}. These results suggest that the addition of OS and the subsequent crosslinking leads mainly to insoluble protein aggregates so that the remainder can only be washed out in small quantities. This finding was also confirmed macroscopically as films crosslinked with OS kept their intrinsic structure after soaking for 24 h, whereas the LPI control films partly disintegrated.

SDS-PAGE analysis of non-crosslinked and crosslinked samples under reducing conditions are shown in Figure 6. The protein bands were assigned to conglutins α, β, and δ according to literature.[13,55,56] Conglutin α is composed of three subunits connected non-covalently, with each exhibiting sizes of 64, 72, and 85 kDa. The subunits are further divided into alkaline polypeptides of 21–24 kDa and acidic polypeptides of 42–62 kDa linked together via intermolecular disulfide bonds. Conglutin β is the only lupin protein free of disulfide bonds; the sizes of the subunits range from 20 to 70 kDa, each composed of 10–12 distinct and mostly glycosylated polypeptides. Conglutin δ is the smallest protein in lupin seeds,

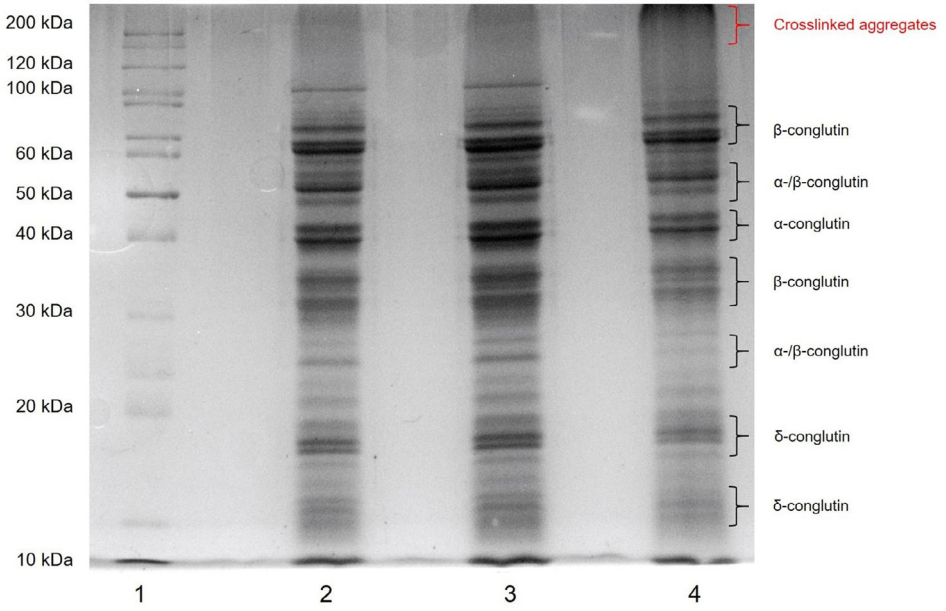

FIGURE 6 SDS-PAGE of LPI with and without the addition of OS. Lanes were loaded as follows: 1 = protein ladder; 2 = freeze-dried LPI; 3 = precipitated LPI; 4 = crosslinked with OS and precipitated LPI. LPI, lupin protein isolate; OS, oxidized sucrose; SDS-PAGE, sodium dodecyl sulfate-polyacrylamide gel electrophoresis. [Color figure can be viewed at wileyonlinelibrary.com]

comprising subunits between 10 and 20 kDa. In lane 3, a strong protein band above 200 kDa can be observed, this supports the formation of crosslinked aggregates with increased molecular weight. The fact that certain protein bands are considerably weaker and some bands even vanished (~100 kDa and ~20 kDa) suggests their participation in the crosslinking aggregates. As the crosslinking is only shown exemplary here, the crosslinking in the produced films cannot be described completely.

In the biodegradation test, the completely mineralized carbon contents of the samples were quantified as CO_2. The cumulative biodegradation of α-cellulose, LPI control film, and LPI/OS100 film are plotted in a diagram, shown in Figure 7. We chose to investigate the LPI/OS100 film as we expected a major impact on biodegradation due to the high OS concentration. α-Cellulose, as positive reference material, presented increasing degradation throughout the experiment, reaching a cumulative biodegradation value of 62% after 91 days according to the released amount of CO_2. The LPI control film reached a maximum of 82%, which is slightly lower than the cumulative biodegradation of 100% in 90 days, which we already showed in a previous study using a respirometric system.[57] The biodegradation value of the LPI/OS100 film was determined to 70% after 91 days. CO_2 release curves typically show a lag phase, a biodegradation phase, and a plateau phase.[58] While the lag and biodegradation phases are present in the curve of α-cellulose, the plateau phase has not yet been reached after 91 days. The curves of both lupin protein-based films showed no lag phases and reached their plateau phase after about 3 weeks. Generally, the biodegradation of protein-based materials is faster and more complete than other biopolymers. It consists of a two-stage process: First, hydrolytic enzymes break down the protein into short-chain polypeptides and amino acids. Amino acids are a nutritious source for the microbiome and join several metabolic processes involving different enzymes.[59] A high solubility of proteins in water further promotes accessibility by microorganisms. As we showed that the TSM of the LPI/OS100 film was significantly reduced (Table 1), a lower biodegradation compared with the LPI control film can be explained. Nevertheless, both films based on LPI show high cumulative biodegradation values after 91 days and can be termed highly biodegradable.

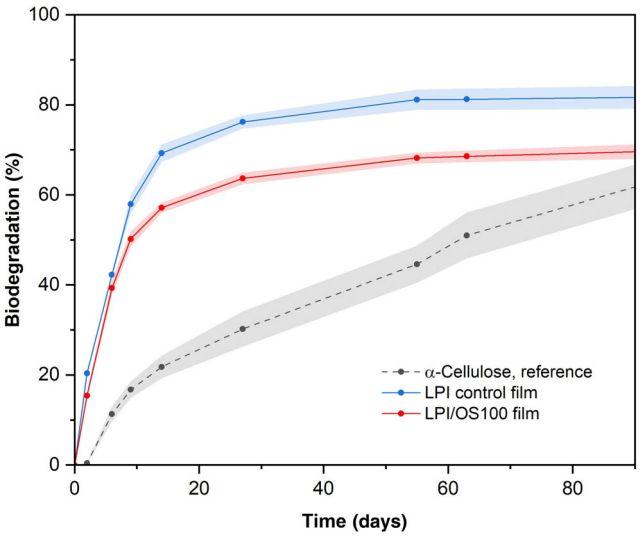

FIGURE 7 Cumulative biodegradation with standard deviations (color shading) of LPI film and LPI/OS100 film. LPI, lupin protein isolate, OS, oxidized sucrose. [Color figure can be viewed at wileyonlinelibrary.com]

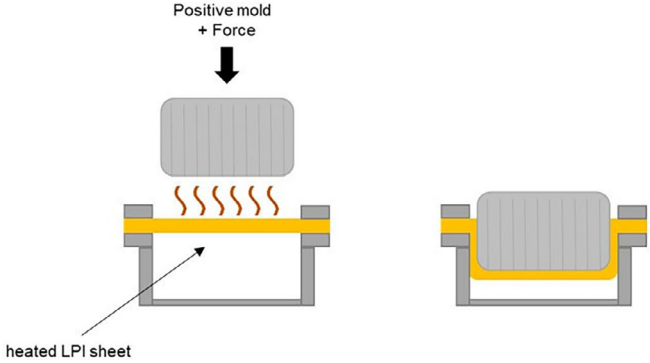

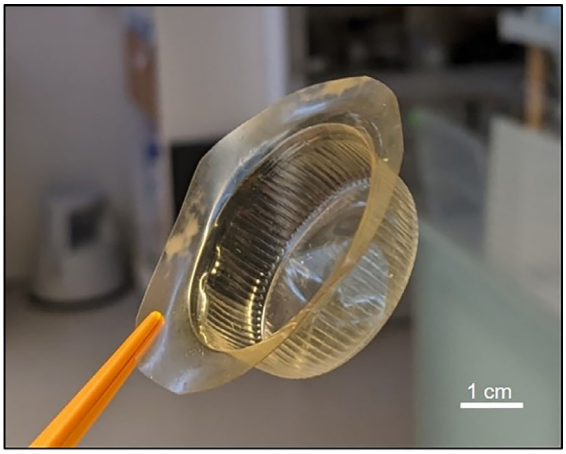

FIGURE 8 Schematic of thermoforming process and a produced component based on LPI. LPI, lupin protein isolate. [Color figure can be viewed at wileyonlinelibrary.com]

3.4 | Thermoforming of LPI films

We further demonstrate the potential of crosslinked and non-crosslinked LPI films or sheets for polymer processing technology. Deep-drawing or thermoforming refers to the process of transforming a plastic sheet into a three-dimensional shape by using heat, vacuum, and/or pressure. Figure 8 shows the basic principle of plug-assisted thermoforming and a photograph of a produced component made from LPI film crosslinked with 50 mg g^{-1} OS. In general, only thermoplastic polymers can be processed by thermoforming. It is therefore quite surprising that LPI films crosslinked with OS can also be thermoformed and components can be obtained. Presumably, a low degree of cross-linking and the addition of glycerol and water allow the material to soften at elevated temperatures. Thermoforming can impact several material properties, such as thickness in walls, corners, and bottom, mechanical and optical properties, and particularly gas permeability.[60] The extent to which the properties of crosslinked and non-crosslinked LPI films are influenced by this process must be investigated in detail in the future. Nevertheless, this process extends the application range for plant protein-based materials.

4 | CONCLUSION

In this experimental study, films based on LPI, obtained from bitter narrow-leaved lupins, and OS were produced by film casting. The addition of a bio-based crosslinker induces crosslinking reactions between OS and protein chains, which significantly affect the mechanical and functional properties of LPI films. Obtained LPI films were strong and ductile with a maximum R_m of 9.3 MPa and a maximum A_t value of 176%. Film solubility was decreased by around 30%, making these films more resistant to moisture. These findings and the results from SDS-PAGE and Bradford assay indicate the formation of an insoluble high molecular protein network that cause these altered properties. We showed that lupin protein, a rather unknown renewable resource for material usage, is suitable for manufacturing thermoformable bioplastic films with improved properties. Additionally, we demonstrated their excellent biodegradability, as films produced with 100 mg g^{-1} OS degraded by around 70% after 91 days. Further research is needed to gain more insight into the structural properties and crosslinking mechanisms of plant proteins for material production. In addition, a detailed characterization of the thermal properties of the produced LPI films with respect to polymer processing technologies is mandatory.

AUTHOR CONTRIBUTIONS

Maximilian Maidl: Conceptualization (lead); data curation (lead); formal analysis (lead); investigation (lead); methodology (lead); validation (lead); visualization (lead); writing – original draft (lead). **Heidi Englberger:** Conceptualization (supporting); investigation (supporting); methodology (supporting). **Amirhossein Abbasnia:** Conceptualization (supporting); investigation (supporting); methodology (supporting). **Daniel Van Opdenbosch:** Conceptualization (supporting); formal analysis (supporting); methodology (supporting). **Cordt Zollfrank:** Funding acquisition (lead); project administration (lead); supervision (lead); writing – review and editing (lead).

ACKNOWLEDGMENTS

This work was supported by the Bavarian Ministry of Food, Agriculture and Forestry through financing within the project "Luprotec" relating to regionally produced lupin protein for the production of bioplastics. Special thanks to Dr. Fred Eickmeyer and the ESKUSA GmbH for the seed provision and the good collaboration. We would also like to thank Lennart Hofmann for his support and ideas during his bachelor's thesis at the Chair for Biogenic Polymers at TUM Campus Straubing for Biotechnology and Sustainability. Open Access funding enabled and organized by Projekt DEAL.

DATA AVAILABILITY STATEMENT

The data that support the findings of this study are available from the corresponding author upon reasonable request.

ORCID

Maximilian Maidl https://orcid.org/0000-0002-5057-7954
Cordt Zollfrank https://orcid.org/0000-0002-2717-4161

REFERENCES

[1] M. A. Da Silva, A. C. K. Bierhalz, in *Handbook of Biopolymers* (Eds: S. Thomas, A. R. Ajitha, C. J. Chirayil, B. Thomas), Springer Nature Singapore, Singapore **2022**, p. 1.
[2] B. Cuq, N. Gontard, S. Guilbert, *Cereal Chem.* **1998**, *75*, 1.
[3] L. Wang, X. Ji, Y. Cheng, Y. Tao, J. Lu, J. Du, H. Wang, *Int. J. Biol. Macromol.* **2022**, *223*, 120.
[4] M. Amirkhani, A. N. Netravali, W. Huang, A. G. Taylor, *Hortscience* **2016**, *51*, 1121.
[5] M. Hadidi, S. Jafarzadeh, M. Forough, F. Garavand, S. Alizadeh, A. Salehabadi, A. M. Khaneghah, S. M. Jafari, *Trends Food Sci. Technol.* **2022**, *120*, 154.
[6] H. Chen, J. Wang, Y. Cheng, C. Wang, H. Liu, H. Bian, Y. Pan, J. Sun, W. Han, *Polymer* **2019**, *11*, 12.
[7] A. Lamp, M. Kaltschmitt, J. Dethloff, *Molecules* **2022**, *27*, 446.
[8] W.-S. Choi, J. H. Han, *J. Food Sci.* **2001**, *66*, 319.

[9] B. Ghanbarzadeh, A. R. Oromiehi, *Int. J. Biol. Macromol.* **2008**, *43*, 209.
[10] N. Gontard, S. Guilbert, J.-L. Cuq, *J. Food Sci.* **1993**, *58*, 206.
[11] H. Tian, G. Guo, X. Fu, Y. Yao, L. Yuan, A. Xiang, *Int. J. Biol. Macromol.* **2018**, *120*, 475.
[12] M. Yamada, S. Morimitsu, E. Hosono, T. Yamada, *Int. J. Biol. Macromol.* **2020**, *149*, 1077.
[13] S. Shrestha, L. Van't Hag, V. S. Haritos, S. Dhital, *Trends Food Sci. Technol.* **2021**, *116*, 928.
[14] J. Berghout, R. M. Boom, A. J. van der Goot, *Food Hydrocoll.* **2015**, *43*, 465.
[15] I. M. Sousa, J. R. Mitchell, D. A. Ledward, S. E. Hill, M. L. da Costa, *Z. Lebensm. Unters. Forsch.* **1995**, *201*, 566.
[16] P. Gulewicz, C. Martínez-Villaluenga, J. Frias, D. Ciesiołka, K. Gulewicz, C. Vidal-Valverde, *Food Chem.* **2008**, *107*, 830.
[17] P. Chew, *Food Chem.* **2003**, *83*, 575.
[18] C. Burgos-Diaz, M. Opazo Navarrete, T. Wandersleben, M. Soto-Añual, T. Barahona, M. Bustamante, *Plant Foods Hum. Nutr.* **2019**, *74*, 508.
[19] P. Guerrero, P. M. Stefani, R. A. Ruseckaite, K. de La Caba, *J. Food Eng.* **2011**, *105*, 65.
[20] A. Chango, C. Villaume, H. Bau, J. Nicolas, L. Mejean, *Food Res. Int.* **1995**, *28*, 91.
[21] E. J. Hopkins, A. K. Stone, J. Wang, D. R. Korber, M. T. Nickerson, *J. Texture Stud.* **2019**, *50*, 539.
[22] M. Alsadi, I. Al-Anbari, *Indian J. Ecol.* **2021**, *48*, 174.
[23] H. M. Azeredo, K. W. Waldron, *Trends Food Sci. Technol.* **2016**, *52*, 109.
[24] A. Kamada, M. Rodriguez-Garcia, F. S. Ruggeri, Y. Shen, A. Levin, T. P. J. Knowles, *Nat. Commun.* **2021**, *12*, 3529.
[25] A. González, G. Gastelú, G. N. Barrera, P. D. Ribotta, C. I. Álvarez Igarzabal, *Food Hydrocoll.* **2019**, *89*, 758.
[26] E. A. Soliman, M. S. Tawfik, H. El-Sayed, Y. G. Moharram, *Am. J. Food Technol.* **2007**, *2*, 462.
[27] C. Protano, G. Buomprisco, V. Cammalleri, R. N. Pocino, D. Marotta, S. Simonazzi, F. Cardoni, M. Petyx, S. Iavicoli, M. Vitali, *Cancers* **2021**, *14*, 1.
[28] H. Kono, J. Noda, H. Wakamori, *Molecules* **2022**, *27*, 18.
[29] A. O. Kalu, E. C. Egwim, A. Jigam, H. L. Muhammad, *Nano Express* **2022**, *3*, 10.
[30] B. Mu, L. Xu, Y. Yang, *Ind. Crops Prod.* **2021**, *173*, 114109.
[31] P. Liu, H. Xu, X. Mi, L. Xu, Y. Yang, *Macromol. Mater. Eng.* **2015**, *300*, 414.
[32] P. Liu, Z. Zhou, B. Mu, *J. Mater. Sci.* **2022**, *57*, 19502.
[33] B. Jayachandran, T. N. Parvin, M. M. Alam, K. Chanda, *Molecules* **2022**, *27*, 8124.
[34] E. A. Hoffman, B. L. Frey, L. M. Smith, D. T. Auble, *J. Biol. Chem.* **2015**, *290*, 26404.
[35] S. Farris, J. Song, Q. Huang, *J. Agric. Food Chem.* **2010**, *58*, 998.
[36] H. A. Al-Ali, U. Shah, M. J. Hackett, M. Gulzar, E. Karakyriakos, S. K. Johnson, *Innov. Food Sci. Emerg. Technol.* **2021**, *68*, 102634.
[37] R. E. Wing, J. L. Willett, *Ind. Crops Prod.* **1997**, *7*, 45.
[38] L. A. Kunte, A. Gennadios, S. L. Cuppett, M. A. Hanna, C. L. Weller, *Cereal Chem. J.* **1997**, *74*, 115.
[39] F. Eckel, K. Sinzinger, D. van Opdenbosch, D. Schieder, V. Sieber, C. Zollfrank, *Biodegradation* **2023**, *35*, 1.
[40] I. Muranyi, C. Otto, C. Pickardt, P. Koehler, U. Schweiggert-Weisz, *Food Res. Int.* **2013**, *54*, 1419.
[41] E. Sironi, F. Sessa, M. Duranti, *Eur. Food Res. Technol.* **2005**, *221*, 145.
[42] C. Wang, L. Jiang, D. Wei, Y. Li, X. Sui, Z. Wang, D. Li, *Procedia Eng.* **2011**, *15*, 4819.
[43] P. Nahimana, A. D. Kerezsi, G. Karamoko, H. Abdelmoumen, C. Blecker, R. Karoui, *Eur. Food Res. Technol.* **2023**, *249*, 2387.
[44] D. de Wit, R. van den Berg, L. A. Johansson, F. van Rantwijk, L. Maat, A. P. Kieboom, *Carbohydr. Res.* **1992**, *226*, 253.
[45] M. Feng, X. Hu, Y. Yin, Y. Liang, J. Niu, J. Yao, *Polymer* **2022**, *14*, 14.
[46] H. Kchaou, N. Benbettaieb, M. Jridi, M. Nasri, F. Debeaufort, *Food Hydrocoll.* **2019**, *97*, 105196.
[47] A. Gennadios, H. J. Park, C. L. Weller, *Trans. ASAE* **1993**, *36*, 1867.
[48] R. de Carvalho, C. Grosso, *Food Hydrocoll.* **2004**, *18*, 717.
[49] W. Liu, M. Pellegrini, X. Wang, *Sci. Rep.* **2014**, *4*, 5739.
[50] M. Bukartyk, O. Zholobko, X.-F. Wu, *ACS Omega* **2022**, *7*, 5883.
[51] H. Zhang, L. Wang, H. Li, Y. Chi, H. Zhang, N. Xia, Y. Ma, L. Jiang, X. Zhang, *Foods* **2021**, *10*, 8.
[52] R. W. Nunes, J. R. Martin, J. F. Johnson, *Polym. Eng. Sci.* **1982**, *22*, 205.
[53] G. Levita, S. de Petris, A. Marchetti, A. Lazzeri, *J. Mater. Sci.* **1991**, *26*, 2348.
[54] J. Zink, T. Wyrobnik, T. Prinz, M. Schmid, *Int. J. Mol. Sci.* **2016**, *17*, 1376.
[55] I. S. Muranyi, D. Volke, R. Hoffmann, P. Eisner, T. Herfellner, M. Brunnbauer, P. Koehler, U. Schweiggert-Weisz, *Food Chem.* **2016**, *207*, 6.
[56] K. Grasberger, M. Hammershøj, M. Corredig, *Food Hydrocoll.* **2023**, *138*, 108485.
[57] P. Wolf, M. Reimer, M. Maier, C. Zollfrank, *Polym. Degrad. Stab.* **2023**, *217*, 110538.
[58] J. H. Song, R. J. Murphy, R. Narayan, G. B. H. Davies, *Philos. Trans. R. Soc. Lond. B Biol. Sci.* **2009**, *364*, 2127.
[59] Y. Tachibana, S. Darbe, S. Hayashi, A. Kudasheva, H. Misawa, Y. Shibata, K.-I. Kasuya, *Sci. Rep.* **2021**, *11*, 242.
[60] M. Beltrão, M. Silva, J. C. Viana, F. M. Duarte, D. Dias, R. Marques, S. Cruz, P. Costa, V. Paulo, *Int. J. Mater. Form.* **2024**, *17*, 4.

How to cite this article: M. Maidl, H. Englberger, A. Abbasnia, D. Van Opdenbosch, C. Zollfrank, *J. Appl. Polym. Sci.* **2024**, *141*(42), e56109. https://doi.org/10.1002/app.56109